

Two Heptacopper(II) Disk Complexes with a $[\text{Cu}_7(\mu_3\text{-OH})_4(\mu\text{-OR})_2]^{8+}$ Core

James J. Henkelis,[†] Leigh F. Jones,^{†,‡} Marcelo P. de Miranda,[†] Colin A. Kilner,[†] and Malcolm A. Halcrow^{*†}

[†]*School of Chemistry, University of Leeds, Woodhouse Lane, Leeds LS2 9JT, U.K., and*

[‡]*School of Chemistry, NUI Galway, University Road, Galway, Ireland*

Received August 26, 2010

The reaction of CuX_2 ($\text{X}^- \neq \text{F}^-$) salts with 1 equiv of 3-pyridyl-5-*tert*-butylpyrazole (HL) in basic methanol yields blue solids, from which disk complexes of the type $[\text{Cu}_7(\mu_3\text{-OH})_4(\mu\text{-OR})_2(\mu\text{-L})_6]^{2+}$ and/or the cubane $[\text{Cu}_4(\mu_3\text{-OH})_4(\text{HL})_4]^{4+}$ can be isolated by recrystallization under the appropriate conditions. Two of the disk complexes have been prepared in crystalline form: $[\text{Cu}_7(\mu_3\text{-OH})_4(\mu\text{-OCH}_2\text{CF}_3)_2(\mu\text{-L})_6][\text{BF}_4]_2$ (**2**) and $[\text{Cu}_7(\mu_3\text{-OH})_4(\mu\text{-OCH}_3)_2(\mu\text{-L})_6]\text{Cl}_2 \cdot x\text{CH}_2\text{Cl}_2$ (**3** · $x\text{CH}_2\text{Cl}_2$). The molecular structures of both compounds as solvated crystals can be described as $[\text{Cu}_7(\mu_3\text{-OH})_4(\mu\text{-OR})_2(\mu\text{-L})_6]^{2+}$ ($\text{R} = \text{CH}_2\text{CF}_3$ or CH_3) adducts. The $[\text{Cu}_6(\mu\text{-OH})_4(\mu\text{-OR})_2(\mu\text{-L})_6]$ ring is constructed of six square-pyramidal Cu ions, linked by 1,2-pyrazolido bridges from the L[−] ligands and by basal, apical-bridging hydroxy or alkoxy groups, while the central Cu ion is bound to the four metallamacrocyclic hydroxy donors in a near-regular square-planar geometry. The L[−] ligands project above and below the metal ion core, forming two bowl-shaped cavities that are fully ($\text{R} = \text{CH}_2\text{CF}_3$) or partially ($\text{R} = \text{CH}_3$) occupied by the alkoxy R substituents. Variable-temperature magnetic susceptibility measurements on **2** demonstrated antiferromagnetic interactions between the Cu ions, yielding a spin-frustrated $S = 1/2$ magnetic ground state that is fully populated below around 15 K. Electrospray ionization mass spectrometry, UV/vis/near-IR, and electron paramagnetic resonance measurements imply that the heptacopper(II) disk motif is robust in organic solvents.

Introduction

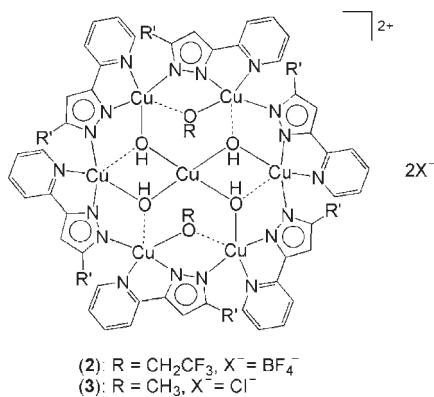
During our continuing studies into the supramolecular chemistry of metal/pyrazole derivatives,^{1,2} we have reported cyclic hexanuclear complexes based on 3-pyridyl-5-*tert*-butylpyrazole (LH).^{3–5} These include $[\text{Cu}_6(\mu\text{-F})_6(\mu\text{-L})_6]$ (**1**), which can bind Na^+ , K^+ , or NH_4^+ at the center of its $[\text{Cu}_6(\mu\text{-F})_6]^{6+}$ ring,^{3,4} like a traditional (inverse) metallacrown,⁶ but also possesses two chiral cavities formed by the L[−] ligands. The cavities project above and below the metal core, and each has three F[−] hydrogen-bond acceptors at its base. The cavities can bind a range of alkylammonium cations through N–H···F hydrogen bonding, including zwitterionic amino acids.⁴ While pursuing new compounds from this chemistry, we have isolated two heptacopper(II) complexes

with a metal-centered disk structure (Chart 1). This homometallic disk motif is best known in manganese,^{7,8} iron,^{8,9} cobalt,¹⁰ and polyoxometallate¹¹ chemistry, but there are also disk complexes containing other first-row transition-metal ions,^{12,13} as well as heterometallic examples.^{11,14} Only two heptanuclear copper(II) complexes with disk structures have been reported previously, however, which both have connectivities and coordination geometries different from those in Chart 1.¹³ Other known heptacopper(II) complexes have vertex-sharing double-cubane structures¹⁵ or more irregular topologies.¹⁶

*To whom correspondence should be addressed. E-mail: m.a.halcrow@leeds.ac.uk. Tel.: (+44) 113 343 6506. Fax: (+44) 113 343 6565.

- (1) Halcrow, M. A. *Dalton Trans.* **2009**, 2059.
- (2) (a) Renard, S. L.; Kilner, C. A.; Fisher, J.; Halcrow, M. A. *J. Chem. Soc., Dalton Trans.* **2002**, 4206. (b) Renard, S. L.; Sylvestre, I.; Barrett, S. A.; Kilner, C. A.; Halcrow, M. A. *Inorg. Chem.* **2006**, *45*, 8711. (c) Jones, L. F.; Camm, K. D.; Kilner, C. A.; Halcrow, M. A. *CrystEngComm* **2006**, *8*, 719.
- (3) Day, J.; Marriott, K. E. R.; Kilner, C. A.; Halcrow, M. A. *New J. Chem.* **2010**, *34*, 52.
- (4) Jones, L. F.; Kilner, C. A.; de Miranda, M. P.; Wolowska, J.; Halcrow, M. A. *Angew. Chem., Int. Ed.* **2007**, *46*, 4073.
- (5) Jones, L. F.; Barrett, S. A.; Kilner, C. A.; Halcrow, M. A. *Chem.—Eur. J.* **2008**, *14*, 223.
- (6) Jones, L. F.; Kilner, C. A.; Halcrow, M. A. *Chem.—Eur. J.* **2009**, *15*, 4667.
- (7) Mezei, G.; Zaleski, C. M.; Pecoraro, V. L. *Chem. Rev.* **2007**, *107*, 4933.

- (7) For example, see: (a) Abbati, G. L.; Cornia, A.; Fabretti, A. C.; Caneschi, A.; Gatteschi, D. *Inorg. Chem.* **1998**, *37*, 3759. (b) Harden, N. C.; Bolcar, M. A.; Wernsdorfer, W.; Abboud, K. A.; Streib, W. E.; Christou, G. *Inorg. Chem.* **2003**, *42*, 7067. (c) Chakov, N. E.; Wernsdorfer, W.; Abboud, K. A.; Christou, G. *Inorg. Chem.* **2004**, *43*, 5919. (d) Saalfrank, R. W.; Nakajima, T.; Mooren, N.; Scheurer, A.; Maid, H.; Hampel, F.; Trieflinger, C.; Daub, J. *Eur. J. Inorg. Chem.* **2005**, 1149. (e) Saalfrank, R. W.; Scheurer, A.; Prakash, R.; Heinemann, F. W.; Nakajima, T.; Hampel, F.; Leppin, R.; Pilawa, B.; Rupp, H.; Müller, P. *Inorg. Chem.* **2007**, *46*, 1586. (f) Koizumi, S.; Nihei, M.; Shiga, T.; Nakano, M.; Nojiri, H.; Bircher, R.; Waldmann, O.; Ochsenbein, S. T.; Güdel, H. U.; Fernandez-Alonso, F.; Oshio, H. *Chem.—Eur. J.* **2007**, *13*, 8445.
- (8) Liu, T.; Wang, B.-W.; Chen, Y.-H.; Wang, Z.-M.; Gao, S. Z. *Anorg. Allg. Chem.* **2008**, *634*, 778.
- (9) (a) Oshio, H.; Hoshino, N.; Ito, T.; Nakano, M.; Renz, F.; Gütllich, P. *Angew. Chem., Int. Ed.* **2003**, *42*, 223. (b) Hoshino, N.; Ako, A. M.; Powell, A. K.; Oshio, H. *Inorg. Chem.* **2009**, *48*, 3396. (c) Labat, G.; Bosovic, C.; Güdel, H. U. *Acta Crystallogr., Sect. E* **2005**, *61*, m611.
- (10) Murrie, M. *Chem. Soc. Rev.* **2010**, *39*, 1986 and references cited therein.

Chart 1. New Disk Complexes Described in This Work ($R' = \text{tert-Butyl}$)^a

^aThe dashed lines show the longer apical Cu–O bonds at the square-pyramidal Cu^{II} centers.

Experimental Section

General Information. All reactions were carried out in air, using nonpredried AR-grade solvents. 3{5}-(Pyrid-2-yl)-5{3}-tert-butylpyrazole (LH) was prepared in two steps following literature procedures: Claisen condensation of ethyl picolinate

(11) Many compounds based on the anions $[\text{MMo}_6\text{O}_{24}]^{m-}$ ($M = \text{Mo}$ or another metal) have been reported. For example, see: (a) Ohashi, Y.; Yanagi, K.; Sasada, Y.; Yamase, T. *Bull. Chem. Soc. Jpn.* **1992**, *55*, 1254. (b) Hasenkopf, B.; Delmont, R.; Herson, P.; Gouzerh, P. *Eur. J. Inorg. Chem.* **2002**, 1081. (c) Marcoux, P. R.; Hasenkopf, B.; Vaissermann, J.; Gouzerh, P. *Eur. J. Inorg. Chem.* **2003**, 2406. (d) Liu, C.-M.; Huang, Y.-H.; Zhang, D.-Q.; Gao, S.; Jiang, F.-C.; Zhang, J.-Y.; Zhu, D.-B. *Cryst. Growth Des.* **2005**, *5*, 1531. (e) Coué, V.; Dessapt, R.; Bujoli-Doeuff, M.; Evain, M.; Jobic, S. *Inorg. Chem.* **2007**, *46*, 2824. (f) Song, Y.-F.; Long, D.-L.; Kelly, S. F.; Cronin, L. *Inorg. Chem.* **2008**, *47*, 9137. (g) Song, Y.-F.; McMillan, N.; Long, D.-L.; Thiel, J.; Ding, Y.; Chen, H.; Gadegaard, N.; Cronin, L. *Chem.—Eur. J.* **2008**, *14*, 2349.

(12) (a) Day, V. W.; Eberspacher, T. A.; Klemperer, W. G.; Park, C. W.; Rosenberg, F. S. *J. Am. Chem. Soc.* **1991**, *113*, 8190. (b) Tesmer, M.; Müller, B.; Vahrenkamp, H. *Chem. Commun.* **1997**, 721. (c) Biechel, F.; Dubuc, J.; Henry, M. *New J. Chem.* **2004**, 28, 764. (d) Mitsumoto, K.; Nihei, M.; Shiga, T.; Oshio, H. *Chem. Lett.* **2008**, 37, 966. (e) Meally, S. T.; McDonald, C.; Karotsis, G.; Papaefstathiou, G. S.; Brechin, E. K.; Dunne, P. W.; McArdle, P.; Power, N. P.; Jones, L. F. *Dalton Trans.* **2010**, 39, 4809.

(13) (a) Blake, A. J.; Gould, R. O.; Grant, C. M.; Milne, P. E. Y.; Reed, D.; Winpenny, R. E. P. *Angew. Chem., Int. Ed. Engl.* **1994**, *33*, 195. (b) Tandon, S. S.; Bunge, S. D.; Thompson, L. K. *Chem. Commun.* **2007**, 798.

(14) For example, see: (a) Caneschi, A.; Cornia, A.; Lippard, S. J. *Angew. Chem., Int. Ed. Engl.* **1995**, *34*, 467. (b) Caneschi, A.; Cornia, A.; Fabretti, A. C.; Foner, S.; Gatteschi, D.; Gatteschi, R.; Schenetti, L. *Chem.—Eur. J.* **1996**, *2*, 1379. (c) Abbati, G. L.; Brunel, L.-C.; Casalta, H.; Cornia, A.; Fabretti, A. C.; Gatteschi, D.; Hassan, A. K.; Jansen, A. G. M.; Maniero, A. L.; Pardi, L.; Paulsen, C.; Segre, U. *Chem.—Eur. J.* **2001**, *7*, 1796. (d) Antolini, F.; Hitchcock, P. B.; Lappert, M. F.; Wei, X.-H. *Organometallics* **2003**, *22*, 2505. (e) Tasiopoulos, A. J.; O'Brien, T. A.; Abboud, K. A.; Christou, G. *Angew. Chem., Int. Ed.* **2004**, *43*, 345. (f) Saalfrank, R. W.; Prakash, R.; Maid, H.; Hampel, F.; Heinemann, F. W.; Trautwein, A. X.; Bottger, L. H. *Chem.—Eur. J.* **2006**, *12*, 2428. (g) Kermagoret, A.; Braunstein, P. *Dalton Trans.* **2008**, 1564. (h) Liu, C.-M.; Zhang, D.-Q.; Zhu, D. B. *Inorg. Chem.* **2009**, *48*, 792. (i) Biswas, B.; Weyhermüller, T.; Bill, E.; Chaudhuri, P. *Inorg. Chem.* **2009**, *48*, 1524.

(15) (a) Real, J. A.; De Munno, G.; Chiappetta, R.; Julve, M.; Lloret, F.; Journaux, Y.; Colin, J.-C.; Blondin, G. *Angew. Chem., Int. Ed. Engl.* **1994**, *33*, 1184. (b) Triki, S.; Thétiot, F.; Pala, J. S.; Golhen, S.; Clemente-Juan, J. M.; Gómez-García, C. J.; Coronado, E. *Chem. Commun.* **2001**, 2172. (c) Liu, X.; McAllister, J. A.; de Miranda, M. P.; McInnes, E. J. L.; Kilner, C. A.; Halcrow, M. A. *Chem.—Eur. J.* **2004**, *10*, 1827. (d) Igashira-Kamiyama, A.; Fujioka, J.; Mitsunaga, S.; Nakano, M.; Kawamoto, T.; Konno, T. *Chem.—Eur. J.* **2008**, *14*, 9512.

(16) (a) Klufers, P.; Kunte, T. *Z. Anorg. Allg. Chem.* **2004**, 630, 553. (b) Ferrer, S.; Aznar, E.; Lloret, F.; Castiñeiras, A.; Liu-González, M.; Borrás, J. *Inorg. Chem.* **2007**, *46*, 372.

(17) Levine, R.; Sneed, J. K. *J. Am. Chem. Soc.* **1951**, *73*, 5614.

(18) Yu, W.-S.; Cheng, C.-C.; Cheng, Y.-M.; Wu, P.-C.; Song, Y.-H.; Chi, Y.; Chou, P.-T. *J. Am. Chem. Soc.* **2003**, *125*, 10800.

and 3,3-dimethylbutan-2-one,¹⁷ followed by hydrazinolysis of the resultant 4,4-dimethyl-1-(pyrid-2-yl)pentan-1,3-dione.¹⁸

Elemental microanalyses were performed by the University of Leeds School of Chemistry microanalytical service. IR spectra were obtained as Nujol mulls pressed between NaCl windows between 600 and 4000 cm^{-1} , using a Nicolet Avatar 360 spectrophotometer. Electrospray ionization mass spectrometry (ESI MS) spectra were obtained on a Waters ZQ4000 spectrometer, from MeCN feed solutions. Assignments of the mass spectral peaks are tabulated in the Supporting Information, and all mass peaks have the correct isotopic distributions for the proposed assignments. UV/vis/near-IR (NIR) spectra were run on a Perkin-Elmer Lambda 900 spectrophotometer using 1 cm quartz cells and are also presented in the Supporting Information.

Magnetic susceptibility measurements were performed on a Quantum Design SQUID magnetometer, in an applied field of 1000 G. A diamagnetic correction for the sample was estimated from Pascal's constants,¹⁹ a diamagnetic correction for the sample holder and a TIP of $60 \times 10^{-6} \text{ cm}^3 \text{ mol}^{-1}$ per Cu atom were also applied to the data. The Hamiltonian matrix was calculated in the coupled-spins representation, in which it can be made block-diagonal. The blocks were independently diagonalized using MAPLE²⁰ (with the RACAH package for angular momentum algebra²¹), leading to analytical equations for the energies of their eigenstates and their derivatives. These expressions were used in a nonlinear fit of the van Vleck equation to $\chi_{\text{M}}T$, using an iterative procedure based on the Marquadt method.²² No paramagnetic impurity term was included in the analysis. The errors on the fitted parameters, estimated from their reproducibility in other local minima of the fitting process, are $\pm 0.2 \text{ cm}^{-1}$ for J and ± 0.1 for g .

Synthesis of $[\text{Cu}_7(\mu_3\text{-OH})_4(\mu\text{-OCH}_2\text{CF}_3)_2(\mu\text{-L})_6][\text{BF}_4]_2$ (2). A mixture of LH (0.25 g, 1.24 mmol), $\text{Cu}[\text{BF}_4]_2 \cdot 4\text{H}_2\text{O}$ (0.43 g, 1.24 mmol), and NaOH (0.10 g, 1.24 mmol) was stirred in methanol (50 cm^3) overnight, yielding a dark-green solution. This was allowed to evaporate to dryness upon standing under ambient conditions, and the solid residue was extracted with 2,2,2-trifluoroethanol. The slow diffusion of diethyl ether vapor into the filtered solution afforded turquoise single crystals of the bis(diethyl ether) solvate of **2**, which decompose to the solvent-free complex upon drying in vacuo. Yield: 0.16 g, 44%. Calcd for $\text{C}_{76}\text{H}_{92}\text{B}_2\text{Cu}_7\text{F}_{14}\text{N}_{18}\text{O}_6$: C, 43.8; H, 4.44; N, 12.1. Found: C, 43.6; H, 4.45; N, 12.3. IR spectrum (cm^{-1}): 3625 m, 3491 br m, 3086 w, 2724 w, 2693 w, 1611 s, 1567 m, 1541 w, 1405 m, 1331 m, 1272 m, 1250 m, 1224 w, 1205 m, 1065 br vs, 953 w, 864 w, 824 s, 784 s, 752 m, 689 w, 668 m, 644 m, 606 m.

Synthesis of $[\text{Cu}_7(\mu_3\text{-OH})_4(\mu\text{-OME})_2(\mu\text{-L})_6]\text{Cl}_2 \cdot x\text{CH}_2\text{Cl}_2$ ($3 \cdot x\text{CH}_2\text{Cl}_2$, Where $x \approx 4$). The method used was the same as that for **2**, using $\text{CuCl}_2 \cdot 2\text{H}_2\text{O}$ (0.21 g, 1.24 mmol). The solid residue from the evaporated methanolic reaction mixture was extracted into CH_2Cl_2 . Slow diffusion of Et_2O vapor into the filtered solution afforded a blue powder, which sometimes also contained turquoise crystals. In that case, the powder was removed by decantation, leaving a pure crystalline material that was suitable for single-crystal X-ray characterization. Yield: 43 mg, 11%. Calcd for $\text{C}_{78}\text{H}_{102}\text{Cl}_{10}\text{Cu}_7\text{N}_{18}\text{O}_6$: C, 42.8; H, 4.70; N, 11.5; Cl, 16.2. Found: C, 42.5; H, 4.50; N, 11.2; Cl, 17.2. IR spectrum (cm^{-1}): 3626 br w, 3584 m, 3380 br m, 3175 w, 2726 w, 2671 w, 1607 s, 1566 m, 1546 w, 1333 m, 1306 w, 1257 m, 1203 m, 1155 s, 1119 w, 1041 m, 1014 w, 985 w, 936 w, 916 w, 890 w, 776 s, 687 w, 641 w.

(19) O'Connor, C. J. *Prog. Inorg. Chem.* **1982**, *29*, 203.

(20) MAPLE 8, Program for the evaluation of symbolic algebra; Waterloo Maple Inc.: Waterloo, Canada, 2002.

(21) Fritzsche, S.; Inghoff, T.; Bastug, T.; Tomaselli, M. *Comput. Phys. Commun.* **2001**, *139*, 314.

(22) Press, W. H.; Teukolsky, S. A.; Vetterling, W. T.; Flannery, B. P. *Numerical Recipes: the Art of Scientific Computing*; Cambridge University Press: Cambridge, U.K., 1992.

Table 1. Experimental Details for the Crystal Structure Determinations in This Work

	2·2Et ₂ O	3·xCH ₂ Cl ₂ (x = 5.7)
formula	C ₈₄ H ₁₁₂ B ₂ Cu ₇ F ₁₄ N ₁₈ O ₈	C _{79.7} H _{105.4} Cl _{13.4} Cu ₇ N ₁₈ O ₆
fw	2234.32	2331.43
cryst syst	triclinic	trigonal
space group	P $\bar{1}$	R $\bar{3}$
a (Å)	11.1372(8)	30.7871(3)
b (Å)	15.6751(11)	30.7871(3)
c (Å)	16.6996(12)	27.0562(4)
α (deg)	116.003(3)	90
β (deg)	100.297(4)	90
γ (deg)	92.519(4)	120
V (Å ³)	2553.3(3)	22209.3(4)
Z	1	9
T (K)	150(2)	150(2)
D _c (Mg m ⁻³)	1.453	1.569
F(000)	1145	10 696
λ (nm)	0.710 73	0.710 73
μ(Mo Kα) (mm ⁻¹)	1.513	1.900
total data collected	50 436	63 739
indep reflns	11 516	11 287
R _{int}	0.071	0.097
R1, wR2 [I > 2σ(I)]	0.053, 0.140	0.073, 0.200
R1, wR2 (all data)	0.084, 0.158	0.127, 0.227

Single-Crystal X-ray Structure Determinations. The structure determination of 2·2Et₂O was carried out on a Bruker X8 Apex diffractometer, with graphite-monochromated Mo Kα radiation generated by a rotating anode. Diffraction data for 3·xCH₂Cl₂ were measured using a Nonius Kappa CCD area detector diffractometer, using graphite-monochromated Mo Kα radiation (λ = 0.710 73 Å) from a sealed-tube source. Both diffractometers were fitted with an Oxford Cryostream low-temperature device. The data were scaled and merged using SAINT (2·2Et₂O)²³ or DENZO (3·xCH₂Cl₂),²⁴ which allowed the unambiguous assignment of the relevant space group in both cases. The structures in this study were solved by direct methods (SHELXS97²⁵) and developed by cycles of full least-squares refinement on F² and difference Fourier syntheses (SHELXL97²⁵). All crystallographic figures were produced using XSEED,²⁶ which incorporates POVRAY.²⁷ Experimental data for the crystal structures are listed in Table 1.

X-ray Structure Determination of 2·2Et₂O. The asymmetric unit of 2·2Et₂O contains half of a complex cation, with Cu(1) lying on the crystallographic inversion center at 1/2, 0, 1/2, and a BF₄⁻ anion and a diethyl ether molecule, both lying on general positions. No disorder was detected during refinement, and no restraints were applied. All H atoms (including the hydroxy H atoms) were placed in calculated positions and were refined using a riding model. The highest residual Fourier peak of +1.1 e Å⁻³ lies 1 Å from Cu(4).

X-ray Structure Determination of 3·xCH₂Cl₂. The asymmetric unit of 3·xCH₂Cl₂ contains half of a complex molecule, with Cu(1) lying on the inversion center 1/2, 0, 1/2, a wholly occupied 1/6 chloride anion lying on the 3 site 2/3, 1/3, 1/3, and two partial CH₂Cl₂ molecules occupying general positions. The remainder of the asymmetric unit was comprised of an extremely diffuse electron density, which could not be modeled satisfactorily. This was dealt with by using the SQUEEZE routine in PLATON.²⁸ A SQUEEZE analysis of the isotropically refined model located 3864 Å³ of void space per unit cell, which is 17%

of the unit cell volume. This space was occupied by 1891 electrons, corresponding to 210 electrons per formula unit. That is equivalent to 5/3 Cl ions (required for charge neutrality, 30 electrons in total) plus 4.3 dichloromethane molecules (42 electrons each) per formula unit, on top of the 1.4 equiv of dichloromethane that was located in the Fourier map and refined in the final model (see below). This is the formula of the crystal that was used in the density and F(000) calculations.

Two of the three unique *tert*-butyl groups in the molecule are disordered, over the following orientations: C(20A)–C(23A) (occupancy 0.4), C(20B)–C(23B) (occupancy 0.4), and C(20C)–C(23C) (occupancy 0.2); C(50A)–C(53)A (occupancy 0.5) and C(50B)–C(53B) (occupancy 0.5). These were modeled using the refined restraints C–C = 1.54(2) Å and 1,3-C···C = 2.51(2) Å. The two partial CH₂Cl₂ sites are C(55A), Cl(5A), and Cl(5B) (occupancy 0.5) and (C55B), (Cl5C), and (Cl5D) (occupancy 0.2). These were refined using the refined restraints C–Cl = 1.76(2) Å and Cl···Cl = 2.87(2) Å.

All wholly occupied non-H atoms, plus the half-occupied CH₂Cl₂ molecule, were refined anisotropically, and all H atoms were placed in calculated positions and refined using a riding model. Wholly occupied methyl group torsions were allowed to refine freely, while disordered methyl group H atoms were fixed in positions. The highest residual Fourier peak of 2.5 e Å⁻³ is 1.4 Å from Cl(54) and may represent a minor alternative site for this Cl atom. The deepest Fourier hole of -1.5 e Å⁻³ is 0.6 Å from Cu(1).

Results

The reaction of HL with hydrated CuX₂ (X⁻ ≠ F⁻) salts in basic methanol generally yields mixtures of products, including heptacopper disk complexes (Chart 1) and salts of the cubane [Cu₄(μ₃-OH)₄(HL)₄]⁴⁺.²⁹ Moderate yields of the disk structure can be isolated in pure form by recrystallizing the crude product mixtures from 2,2,2-trifluoroethanol/diethyl ether. The BF₄⁻ salt of the resultant product was chosen for full characterization because this forms single crystals of X-ray quality. These have the formula [Cu₇(μ₃-OH)₄(μ-OCH₂CF₃)₂(μ-L)₆][BF₄]₂·2(C₂H₅)₂O (2·2Et₂O; Chart 1). The crystals decompose upon drying in vacuo, giving solvent-free 2. In contrast, recrystallization of these mixtures from chlorinated solvents tends to afford the cubane²⁹ as the major product, making the disk complexes hard to purify by that route. We were able to obtain small amounts of one such compound in a pure form, however, namely, 3·xCH₂Cl₂. Single crystals of this compound contain extensive anion and solvent disorder, with x ≈ 6 from a SQUEEZE analysis.²⁸ The dried material retains most of this solvent, with x ≈ 4 by C, H, N, and Cl microanalysis. Although reproducible microanalyses of fresh crystals of the two compounds could not be obtained owing to partial desolvation, the IR spectra of freshly prepared crystals and dried material were barely distinguishable in both cases. Hence, it is likely that the disk complexes retain their structural integrity upon drying.

The dications in 2 and 3 have essentially the same molecular geometry in the single crystal, with the central Cu(1) atom lying on a crystallographic inversion center in both structures (Figures 1 and 2 and the Supporting Information). The cyclic [Cu₆(μ₃-OH)₄(μ-OR)₂(μ-L)₆] moiety is very comparable to the [Cu₆(μ-F)₆(μ-L)₆] structure of 1, containing six square-pyramidal Cu ions [Cu(2)–Cu(4) and their symmetry equivalents] with τ ≤ 0.18.³⁰ The three N donors from

(23) SAINT; Bruker AXS Inc.: Madison, WI, 2007.

(24) Otwinowski, Z.; Minor, W. *Methods Enzymol.* **1997**, *276*, 307.(25) Sheldrick, G. M. *Acta Crystallogr., Sect. A* **2008**, *64*, 112.(26) Barbour, L. J. *J. Supramol. Chem.* **2001**, *1*, 189.

(27) POVRAY, version 3.5; Persistence of Vision Raytracer Pty. Ltd.: Williamstown, Victoria, Australia, 2002.

(28) Spek, A. L. *J. Appl. Crystallogr.* **2003**, *36*, 7.(29) Jones, L. F.; Kilner, C. A.; Halcrow, M. A. *Polyhedron* **2007**, *26*, 1977.

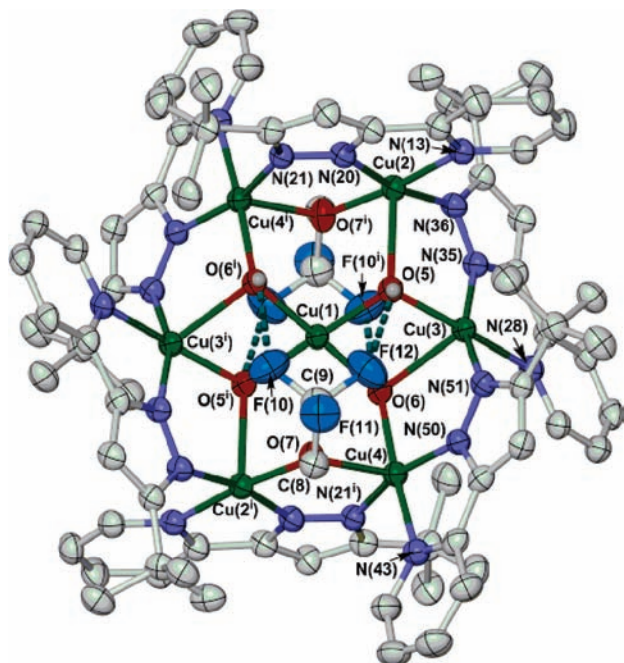


Figure 1. View of the $[\text{Cu}_7(\mu_3\text{-OH})_4(\mu\text{-OCH}_2\text{CF}_3)_2(\mu\text{-L})_6]^{2+}$ cation in $2 \cdot 2\text{Et}_2\text{O}$, showing the atom numbering scheme employed. All C-bound H atoms have been omitted for clarity, and thermal ellipsoids are at the 50% probability level. Symmetry code $i: 1 - x, -y, 1 - z$. Color code: C, white; H, pale gray; Cu, green; F, cyan; N, blue; O, red.

each L^- ligand all occupy basal coordination sites at these metal ions, while the OH^- and OR^- groups bridge between a basal coordination site on one metallacrown Cu ion and the apical coordination site of its neighbor (Chart 1); the $\text{Cu} \cdots \text{O}$ distances to these apical donors are 2.2–2.4 Å. The central Cu ion is bound to the four hydroxyl ligands in a near-regular square-planar geometry. The $\text{Cu}(1) \cdots \text{O}(7)$ distances of 2.941(3) Å in **2** and 2.781(6) Å in **3** (Figures 1 and 2) are too long to be considered significant bonding interactions. The $\text{Cu} \cdots \text{Cu}$ distances within the cyclic $[\text{Cu}_6(\mu_3\text{-OH})_4(\mu\text{-OR})_2]^{6+}$ fragment are 3.3323(8)–3.4783(7) Å, while the $\text{Cu} \cdots \text{Cu}$ distances to Cu(1) are more variable at 3.2056(5)–3.6498(5) Å. Other metric parameters in the two structures are tabulated in the Supporting Information and lie within the usual ranges.

As in **1** and related compounds,^{3–5} the L^- ligands in **2** and **3** form two bowl-shaped cavities of approximate dimensions $2.2 \times 6.0 \times 6.5$ Å (base \times rim \times height), although at least some of this space is taken up by the alkoxide substituents. In **2**, these cavities are fully occupied by the 2,2,2-trifluoroethyl groups, which form weak $\text{O}-\text{H} \cdots \text{F}$ hydrogen bonds with the two hydroxyl groups at the base of each cavity [$\text{O} \cdots \text{F} = 3.040(4)$ and $3.058(4)$ Å; Figure 3]. The cavities in **3** are more open because of its smaller methoxy groups, but disorder in the structure prevented any guest species occupying the cavities from being resolved. Potential in-cavity guests in $3 \cdot x\text{CH}_2\text{Cl}_2$ are dichloromethane,³ water,^{3,5} and/or chloride.

Solid **2** exhibits $\chi_{\text{MT}} = 2.6 \text{ cm}^3 \text{ mol}^{-1} \text{ K}$ at 330 K, slightly less than the theoretical value for seven weakly interacting

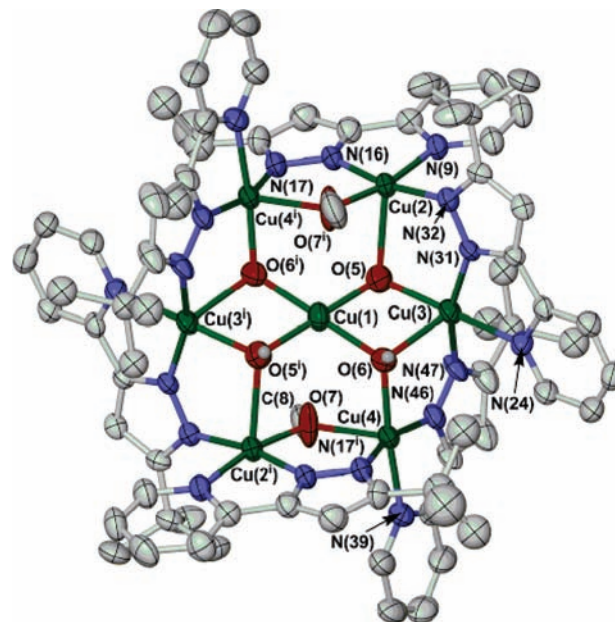


Figure 2. View of the $[\text{Cu}_7(\mu_3\text{-OH})_4(\mu\text{-OMe})_2(\mu\text{-L})_6]^{2+}$ dication in $3 \cdot x\text{CH}_2\text{Cl}_2$, showing the atom numbering scheme employed. For clarity, only one orientation of the disordered *tert*-butyl groups is shown. Other details as given for Figure 1.

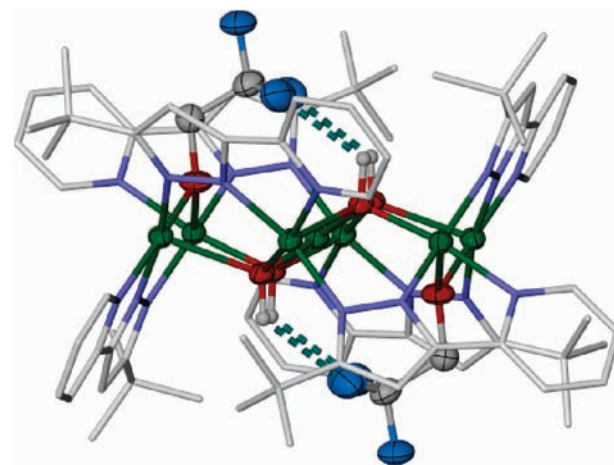


Figure 3. View of the complex dication in $2 \cdot 2\text{Et}_2\text{O}$, showing the 2,2,2-trifluoroethyl groups occupying the bowl-shaped cavities. The atoms of the L^- ligands are deemphasized for clarity, while other atoms have thermal ellipsoids at the 50% probability level, and C-bound H atoms have been omitted. Color code: C (L^-), white; C (CH_2CF_3), gray; H, pale gray; Cu, green; F, cyan; N, blue; O, red.

Cu^{II} ions ($\chi_{\text{MT}} = 2.9 \text{ cm}^3 \text{ mol}^{-1} \text{ K}$ with $g = 2.1$).³¹ As the temperature is lowered, χ_{MT} steadily decreases, plateauing at $0.42(1) \text{ cm}^3 \text{ mol}^{-1} \text{ K}$ below 15 K, which is a typical value for a $S = 1/2$ copper(II) species (Figure 4). Hence, **2** undergoes antiferromagnetic superexchange, giving a $S = 1/2$ magnetic ground state that is almost certainly a consequence of spin frustration at the central Cu(1) ion (Figure 1). In principle, the orientations of the $d_{x^2-y^2}$ magnetic orbitals on the seven Cu ions (Chart 1) mean that six unique J values are required to describe superexchange in **2** (see the Supporting Information). To avoid overparametrization, a simplified $2J$ coupling scheme was used, which only considers basal–basal superexchange pathways between the Cu centers

(30) A perfectly square-pyramidal complex exhibits $\tau = 0$, while a trigonal-bipyramidal metal center gives $\tau = 1$. Addison, A. W.; Rao, T. N.; Reedijk, J.; van Rijn, J.; Verschoor, G. C. *J. Chem. Soc., Dalton Trans.* **1984**, 1349.

(31) Full magnetochemical characterization was only undertaken on **2** because of the difficulty of obtaining bulk samples of $3 \cdot x\text{CH}_2\text{Cl}_2$ in sufficient quantity.

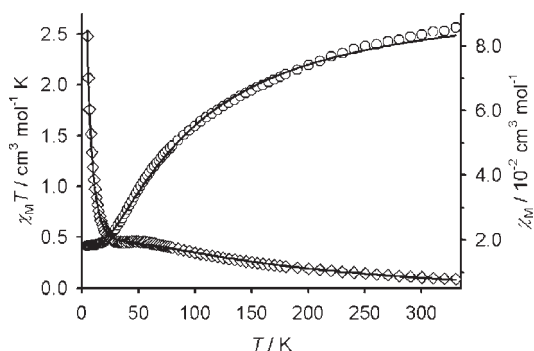


Figure 4. Variable-temperature magnetic susceptibility data from **2** plotted as χ_M (\diamond) and $\chi_M T$ (\circ) vs T . The lines show the calculated data from fit A derived from eq 1. See the text for details.

(eq 1 and the Supporting Information).³²

$$H = -2J_1(S_2 \cdot S_3 + S_3 \cdot S_4 + S_4 \cdot S_{2i} + S_{2i} \cdot S_{3i} + S_{3i} \cdot S_{4i} + S_{4i} \cdot S_2) - 2J_2(S_1 \cdot S_3 + S_1 \cdot S_{3i} + S_1 \cdot S_4 + S_1 \cdot S_{4i}) \quad (1)$$

where S_1 – S_4 and their symmetry equivalents refer to the correspondingly numbered Cu ions in Figure 1. In this model, J_1 describes superexchange between Cu ions in the $[\text{Cu}_6(\mu_3\text{-OH})_4(\mu\text{-OR})_2(\mu\text{-L})_6]$ macrocycle, and J_2 denotes coupling between the metallamacrocycle and the central Cu ion. The $S_1 \cdot S_2/S_1 \cdot S_{2i}$ interaction is neglected because these Cu ions are only linked by one basal, apical bridging group.³² Two sets of parameters were found that model the data almost equally well: $J_1 = -27.4 \text{ cm}^{-1}$, $J_2 = -35.1 \text{ cm}^{-1}$, $g = 2.14$ (fit A); and $J_1 = -43.0$, $J_2 = -0.5 \text{ cm}^{-1}$, $g = 2.12$ (fit B). Fit A is more chemically reasonable, in giving a J_1 value similar to that observed in **1**³ and a significant antiferromagnetic J_2 value. Superexchange across one basal–basal hydroxo bridge, as for J_2 , is expected to be antiferromagnetic for a Cu–O–Cu angle $> 104^\circ$ ³³ [in **2**, Cu(1)–O(5)–Cu(3) = $106.19(12)^\circ$ and Cu(1)–O(6)–Cu(4) = $118.41(13)^\circ$]. Small differences between the observed and calculated $\chi_M T$ vs T data at high temperature may reflect the approximations used in eq 1 (Figure 4).

The lower symmetry coupling scheme in eq 2 was also examined to allow for the differences between the Cu(1)–O(5)–Cu(3) and Cu(1)–O(6)–Cu(4) bridging angles in the crystal structure of **2**· $2\text{Et}_2\text{O}$ (Table 2; see the Supporting Information).

$$H = -2J_1(S_2 \cdot S_3 + S_3 \cdot S_4 + S_4 \cdot S_{2i} + S_{2i} \cdot S_{3i} + S_{3i} \cdot S_{4i} + S_{4i} \cdot S_2) - 2J_2(S_1 \cdot S_3 + S_1 \cdot S_{3i}) - 2J_3(S_1 \cdot S_4 + S_1 \cdot S_{4i}) \quad (2)$$

These different angles might be expected to have a greater effect on the magnetic structure of **2**³³ than the small

(32) Superexchange pathways involving bridging groups bound to apical copper coordination sites are expected to make only a small contribution to the magnetic behavior of the compound.³³

(33) Tercero, J.; Ruiz, E.; Alvarez, S.; Rodríguez-Fortea, A.; Alemany, P. *J. Mater. Chem.* **2006**, *16*, 2729 and references cited therein.

(34) We did not investigate lowering of the magnetic symmetry within the hexacopper ring because the structural variations between the three unique basal–basal Cu–N–N–Cu bridges in **2** are small (Supporting Information) and the magnetic interaction in $[\text{Cu}_2(\mu\text{-pyrazolido})]^{3+}$ moieties is relatively insensitive to small structural differences. Spodine, E.; Atria, A. M.; Valenzuela, J.; Jalocha, J.; Manzur, J.; García, A. M.; Garland, M. T.; Peña, O.; Saillard, J.-Y. *J. Chem. Soc., Dalton Trans.* **1999**, 3029.

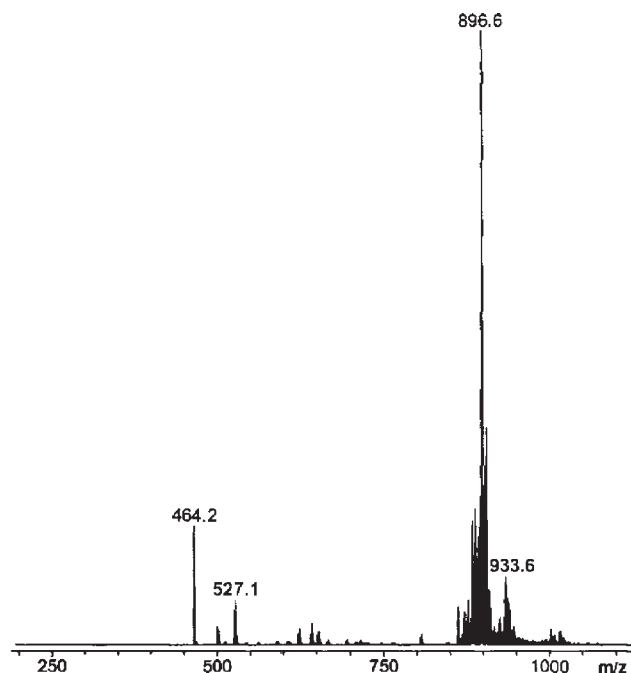


Figure 5. ESI MS spectrum of **3**. An expansion of the spectrum and tabulated peak assignments are given in the Supporting Information.

structural variations between the different $[\text{Cu}_2(\mu\text{-L})]^{3+}$ bridging groups.³⁴ This yielded a fit of the data that was visually indistinguishable to that given by eq 1, with the fitted parameters $J_1 = -27.4 \text{ cm}^{-1}$, $J_2 = -35.3 \text{ cm}^{-1}$, $J_3 = -35.1 \text{ cm}^{-1}$, and $g = 2.14$. The identical values for J_2 and J_3 under this model, within experimental error, lend some support for the approximations used in eq 1.

ESI MS spectra of **2** and **3** from a MeCN solution show strong envelopes of overlapping dicationic molecular ions, which can be assigned to the disk complexes, their solvent adducts, or fragmentation products (see the Supporting Information). The spectrum of **3** contains strong peaks from the intact cluster $[\text{Cu}_7(\text{OH})_4(\text{OMe})_2\text{L}_6]^{2+}$ ($m/z = 887.6$) and the adducts $[\text{Cu}_7(\text{OH})_4(\text{OMe})_2\text{L}_6(\text{solv})]^{2+}$ [solv = H_2O ($m/z = 896.6$), MeOH (903.6), and MeCN (908.6)]; Figure 5 and the Supporting Information]. Additional peaks from the hexahydroxy disk $[\text{Cu}_7(\text{OH})_6\text{L}_6(\text{OH}_2)_n]^{2+}$ [$n = 1$ ($m/z = 882.6$) and 2 (891.6)] are also apparent, along with other weak ions assignable to solvent adducts, sodium formate adducts (from the calibrant in the feed solution), or fragmentation products of **3**. In contrast, the spectrum of **2** is dominated by $[\text{Cu}_7(\text{OH})_4(\text{OCH}_2\text{CF}_3)_2\text{L}_5]^{2+}$ ($m/z = 855.5$), its formate adducts $[\text{Cu}_7(\text{OH})_4(\text{OCH}_2\text{CF}_3)_2\text{L}_5(\text{O}_2\text{CH})_m]^{2+}$ [$m = 1$ (878.6) and 2 (901.6)], and their fragmentation products. The increased tendency of **2** to lose an L^- ligand under these conditions might reflect the steric influence of its trifluoroethoxy substituents, compared to the smaller methoxy groups in **3**. Be that as it may, the degree of fragmentation in the mass spectra of **2** and **3** is much smaller than that for **1** under the same conditions.⁴ Hence, the centrally complexed Cu ion appears to increase the robustness of the $[\text{Cu}_7(\text{OH})_4(\text{OR})_2\text{L}_6]^{2+}$ moiety in the ESI MS experiment.

The solution stability of **2** was also studied by examining its solvatochromism. The d–d maximum exhibited by the complex in CH_2Cl_2 , MeCN, and MeNO₂ shows little variation, at $\lambda_{\text{max}} = 657\text{--}663 \text{ nm}$ ($\epsilon_{\text{max}} = 372\text{--}388 \text{ dm}^3 \text{ mol}^{-1} \text{ cm}^{-1}$ or $54 \text{ dm}^3 \text{ mol}^{-1} \text{ cm}^{-1}$ per Cu ion). Those are typical values for

Cu^{II} centers in tetragonal N/O-donor ligand fields³⁵ and closely resemble the spectra shown by **1** in the same solvents.⁴ The similarity of these three spectra strongly implies that the structure of the compound in all three solvents is the same and, hence, that the disk complex does not undergo significant fragmentation under these conditions. The same d–d transition was slightly red-shifted, broadened, and more intense in a MeOH solution, however, at 680 nm (442 dm³ mol⁻¹ cm⁻¹). In contrast, the UV/vis of **1** in MeOH was almost superimposable on its spectra in these other solvents.⁴ It is uncertain whether the slightly different d–d spectrum of **2** in MeOH is caused by the partial solvolysis of the complex in this medium or whether it reflects hydrogen-bonding interactions between the complex and the MeOH solvent.

Unlike **1**,⁴ **2** does not give an observable ¹H NMR spectrum in CD₂Cl₂ or CD₃CN, reflecting the influence of the additional Cu ion on its magnetic structure. Compound **2** is also electron paramagnetic resonance (EPR)-silent at the X band in the solid state at 115 K and above and in CH₂Cl₂ at room temperature. As a frozen CH₂Cl₂ glass at 115 K, a very broad and slightly unsymmetric Lorentzian peak is observed, centered at *g* = 2.1 with a line width of ca. 2000 G at half-height (see the Supporting Information). That is consistent with the compound existing in a mixture of half-integral spin states at this temperature, as is implied by the solid-state magnetic data. Importantly, the absence of any EPR features assignable to mononuclear copper(II) species is additional evidence that **2** does not undergo significant fragmentation in this solvent.⁴

Conclusions

We have now described two different classes of inverse metallacrown based on the [Cu₆(μ-X)₆(μ-L)₆] motif. When X⁻ = F⁻, the hexacopper complex can be isolated in its guest-free form (compound **1**)³ but will also form the adducts [M_C**1**]⁺ (M⁺ = Na⁺, K⁺, or NH₄⁺) in the solid state when synthesized in the presence of those monocations.^{3,4} The cation guest in these complexes lies at the center of the [Cu₆(μ-F)₆]⁶⁺

ring and is bound to the fluoro donors through dative or hydrogen-bonding interactions. The affinity of **1** for Na⁺ is strong enough to sequester it from pyrex glass.³ Coordination of excess copper to **1** to form [Cu_C**1**]²⁺ has not been observed, however. Conversely, when X⁻ = OR⁻ (R = H and/or alkyl), the free [Cu₆(μ-OR)₆(μ-L)₆] ring is not isolated as the guest-free metallamacrocyclic but can only be crystallized with a guest Cu^{II} ion [Cu_CCu₆(μ-OR)₆(μ-L)₆]²⁺ (**2** and **3**). No adduct [Na_CCu₆(μ-OR)₆(μ-L)₆]⁺ has been isolated, even though sodium is present in these reaction mixtures. The apparently different cation affinities of [Cu₆(μ-X)₆(μ-L)₆] when X = F⁻ and OR⁻ probably reflects the increased hardness of the fluoro donors, which will favor coordination of harder guest species like the alkali-metal cations.

The above behavior can also be compared to the corresponding cobalt compound [Co₆(μ-OH)₆(μ-L)₆]^{*m*+} (*m* = 2 or 3). This is a supramolecular anion host, but unlike the copper systems, it shows no tendency to bind cation guests at its center.⁵ Presumably, coordination of additional cations is disfavored by the positive charge on that inverse metallacrown.

A detailed study of the binding of cations to [Cu₆(μ-X)₆(μ-L)₆] in solution, including guest selectivity and exchange reactions, is hampered by the paramagnetism of the system, which prohibits detailed NMR characterization, and by the insensitivity of the electronic structures of the Cu ions to the presence or absence of guest cations.⁴ Current work is focused on the preparation of diamagnetic analogues of this metallamacrocyclic and of its cobalt-containing congener, which will allow full NMR studies to be undertaken.

Acknowledgment. The authors thank Dr. H. J. Blythe (University of Sheffield, Sheffield, U.K.) for the magnetic susceptibility data. Financial support for this work was provided by the Leverhulme Trust and the University of Leeds.

Supporting Information Available: Additional figures and tables of metric parameters from the crystal structures of **2** and **3**, mass spectrometry, UV/vis/NIR, and EPR data, and crystallographic data in CIF format. This material is available free of charge via the Internet at <http://pubs.acs.org>.

(35) Lever, A. B. P. *Inorganic Electronic Spectroscopy*, 2nd ed.; Elsevier: Amsterdam, The Netherlands, 1984; pp 554–572.